Research Article

Received: 3 September 2024 Revised: 19 November 2024 Published online in Wiley Online Library: 7 December 2024

(wileyonlinelibrary.com) DOI 10.1002/jctb.7794

Comparison between produced Tingui biochar *versus* commercial Norit in the adsorption of acetaminophen and diclofenac: characterization, batch, and fixed bed system

Débora Federici dos Santos,[a*] Wardleison Martins Moreira,[b] Thiago Peixoto de Araújo,[c] Maria Manuel Serrano Bernardo,[d] Isabel Maria de Figueiredo Ligeiro da Fonseca,[d] Indianara Conceição Ostroski,[e] Maria Angélica Simões Dornellas de Barros[b] and Eduardo Falabella Sousa-Aguiar[a]

Abstract

BACKGROUND: In pressing environmental challenges, practical solutions to remove organic contaminants from water are paramount. This study undertook a crucial task of comparing two adsorbents: BT-KOH, synthesized from Tingui bark activated with potassium hydroxide, and Norit commercial carbon. The comparison was based on experimental data from adsorption kinetics and isotherm tests in batch and fixed bed systems, targeting the removal of acetaminophen and diclofenac. Physicochemical characterization analyses of the materials were also conducted to enhance the comparison.

RESULTS: The study's key finding was the superior performance of BT-KOH over Norit in removing acetaminophen and diclofenac. The maximum adsorption capacities for acetaminophen were 357.7 mg g^{-1} for BT-KOH and 226.3 mg g^{-1} for Norit. For diclofenac, these values were 250.6 mg g^{-1} for BT-KOH and 220.9 mg g^{-1} for Norit. This superiority was attributed to BT-KOH's larger specific surface area and higher quantities of oxygen-containing functional groups.

CONCLUSION: The result underscores the importance of considering the physical–chemical composition of materials in the quest for more effective and sustainable water treatment methods.

Keywords: water treatment; pharmaceutical contaminants; adsorbents; characterizations

INTRODUCTION

The daily consumption of micropollutants such as medicines, personal hygiene products, hormones, pesticides, and others has increased significantly in the last decade. This trend has led to the emergence of new substances in surface and groundwater.[1] Acetaminophen and diclofenac, in particular, are drugs with potentially harmful effects on the health of living beings through chronic exposure.[2]

Acetaminophen and diclofenac are the most widely consumed analgesic and anti-inflammatory drugs in the world. Acetaminophen has an estimated average global consumption of 100 tons/year, while diclofenac has over 14 000 tons/year.[3] Most of these micropollutants are not included in any monitoring program, and consequently, their behavioral and ecotoxicological effects are not yet well understood.[4] In this context, the research on the adsorption efficiency of Tingui and Norit carbons in removing acetaminophen and diclofenac from water is of utmost importance.

In addition, these micropollutants are in the aquatic ecosystem in low concentrations, generally ranging from ng to μg L^{-1}. Due to this low concentration, detecting and removing these

* *Correspondence to: DFd Santos. School of Chemistry, Federal University of Rio de Janeiro, Rio de Janeiro, 21941-909, Brazil, E-mail: pg54597@uem.br*

a *School of Chemistry, Federal University of Rio de Janeiro, Rio de Janeiro, Brazil*

b *Department of Chemical Engineering, State University of Maringá, Paraná, Brazil*

c *Department of Chemical Engineering, Federal Technological University of Paraná, Paraná, Brazil*

d *LAQV/REQUIMTE, Department of Chemistry, Faculty of Science and Technology, New University of Lisbon, Caparica, Portugal*

e *Institute of Chemistry, Federal University of Goiás, Goiás, Brazil*

micropollutants by standard water treatment methods becomes difficult, creating a significant challenge to the reuse of treated water and the sustainability of water management.[5] Generally, water and sewage treatment plants aim to remove organic and bacteriological contaminants.[6]

There are various techniques to eliminate micropollutants from water, such as photocatalytic or ultrasonic oxidation, aerobic or anaerobic biodegradation, electrocoagulation, nanofiltration, ozonation, adsorption, and others.[7] Adsorption stands out among these methods, attracting significant attention due to its accessibility, simplicity, effectiveness, and the wide range of materials available as adsorbents.[8] Adsorbent from sugarcane bagasse,[9] Norway spruce bark,[10] banana peel,[11] and coconut shell[12] were used to adsorb acetaminophen. In contrast, palm fibers,[13] *Guazuma ulmifolia* Lam. Fruit,[14] and apricot seed[15] derived adsorbents were used to remove diclofenac from aqueous solutions.

These adsorbent materials are synthesized from various raw materials, which are carbonized at high temperatures in a controlled environment. Carbon activation can be carried out by two main methods: physical activation and chemical activation. Physical activation involves treating carbonized coal with oxidizing agents such as water vapor or carbon dioxide. This process creates pores and increases the surface area of the carbon, resulting in a highly porous material. On the other hand, chemical activation uses chemical agents, such as phosphoric acid or potassium hydroxide, which are applied to the precursor prior to carbonization, facilitating the formation of pores during carbonization. The main difference between the two methods lies in the way the porous structure is developed. Chemical activation tends to produce activated carbons with a wider pore distribution and a larger specific surface area compared to physical activation. This increased porosity and surface area are crucial to the adsorption process as they provide more available sites for interaction with contaminant molecules, improving the efficiency of pollutant removal in water and wastewater treatment applications.[16-18]

Generally, the efficiency of an adsorbent in removing a given adsorbate is determined using batch adsorption processes. However, fixed-bed columns are the most widely used in industry because the contaminated effluent can be treated continuously. In addition, continuous column adsorption allows large volumes of adsorbates to be treated with minimal instantaneous contact between the adsorbed pollutants and the adsorbent bed.[19,20]

In this context, this study aimed to evaluate the adsorption efficiency of a produced Tingui biochar activated with potassium hydroxide (BT-KOH) in removing acetaminophen and diclofenac from aqueous solutions using experimental data obtained from adsorption kinetics and isotherm tests in batch and fixed-bed systems. These data were compared with those of Norit commercial carbon. In addition, both BT-KOH and Norit were characterized using physicochemical techniques to understand their main structural differences.

It should be noted that comparing carbons synthesized from waste raw materials with known commercial carbon is a valuable opportunity to evaluate its properties, performance, and applicability in various fields. Norit is one of the most recognized commercial activated carbons, widely used in industrial and research applications. Its consistent, high-quality performance is a reliable parameter for comparing the effectiveness of new adsorbent materials. Moreover, this commercial carbon is intended to be used for potable water processing, removing a wide range of organic micropollutants. This practice provides a reliable reference point for new materials and drives significant advances in science and technology, leading to the development of more efficient and sustainable products. By comparing these materials, strengths and areas for improvement can be identified in each, stimulating innovation and improving production processes. In addition, this approach facilitates the selection of the most suitable material for a given application, considering factors such as cost, availability, and environmental impact.

Through these comparisons, new ways of optimizing the production of synthesized carbons can be discovered, improving their efficiency and performance in a wide range of applications, from water and air purification to environmental remediation. These advances can benefit the industry and promote more sustainable and environmentally friendly practices. Therefore, by comparing synthesized with commercial carbons we are boosting scientific and technological progress and contributing to a more promising future where natural resources are used more efficiently and responsibly.

MATERIALS AND METHODS

Adsorbents

Preparation of activated Tingui carbon (BT-KOH)

The Tingui bark was pyrolyzed in a reactor placed in a tube furnace at 550 °C for 120 min using a heating rate of 10 °C min and a nitrogen flow of 150 mL min^{-1}. The Tingui carbon obtained by the pyrolytic route was then activated with potassium hydroxide in a ratio of 1:4 (m/V). To do this, 50 g of Tingui carbon was mixed with 200 mL of aqueous KOH solution (1 g mL^{-1}). This mixture was heated at 210 °C for 360 min. The paste formed was dried in an oven at 105 °C for 1440 min. Finally, the dried paste was added to a stainless steel reactor and taken to a tube furnace at 850 °C for 60 min using a heating rate of 10 °C and a nitrogen flow of 150 mL min^{-1}.[21]

Commercial carbon (Norit)

The commercial carbon Norit GAC 1240 W was purchased by Sigma-Aldrich. It is a granular coal, steam-activated, for potable water processing.

Textural and chemical characterization of adsorbents

The Tingui barks, BT-KOH, and Norit were characterized using the methods described in Table 1.

Adsorbates

Acetaminophen and diclofenac (Purity 99%, Merck, Sigma-Aldrich) were quantified using UV–VIS spectrophotometry (Hach DR 5000) at a wavelength of 243 and 275 nm, respectively.

Adsorption kinetics and isotherms

All the adsorption tests were carried out in a batch system under agitation of 150 rpm and a temperature of 25 °C in an orbital shaker.

The adsorption kinetics tests were carried out by adding 50 mL of contaminant solution (acetaminophen or diclofenac, 100 mg L^{-1}) to 20 mg of adsorbent (BT-KOH or Norit) and varying the contact time between the adsorbate and the adsorbent over 2880 min. Equation (1) determined the adsorption capacity of BT-KOH and Norit at a given time t. The experimental data obtained were fitted to the Pseudo-First-Order, Pseudo-Second-Order, and Elovich theoretical models (see Table 3).

Table 1. Characterization methods of Tingui bark, BT-KOH, and Norit

Technique (Equipment)	Objective	Methodology
Nitrogen adsorption/desorption isotherms (Micromeritics ASAP2020 Plus)	Determine the textural properties of the material.	Determine the amount of nitrogen adsorbed at a relative pressure (P/Po) of 0.95.
Thermogravimetric (TG) (TA Instruments thermal analyzer, Discovery series, model TGA 55)	Explore the degradation mechanisms and durability of adsorbent materials.	During the analysis, the samples were heated from 25 to 1000 °C with a heating ramp of 10 C min^{-1} under an atmosphere of synthetic air.
Fourier transform infrared spectroscopy (FTIR) (Thermo Fisher Scientific Inc)	Determine the functional groups on the surface of adsorbent materials.	The functional groups were identified using the KBr wafer method (Vertex 70v, Bruker) in transmittance mode in the 400 to 4000 cm-1 infrared range.
Elemental analysis (Thermo Finnigan—CE Instruments, model Flash EA 1112 CHNS series)	Quantification of the carbon, hydrogen, nitrogen, and sulfur content of adsorbent materials	The oxygen content (O) was calculated using the following difference: O = 100 − C − H − N − S.
pH_{PZC} (pHmeter, Digimed)	Establish the overall net charge balance.	20 mg of the material was mixed in 50 mL of aqueous NaCl solution (0.1 mol L^{-1}) at different initial pH values (2 to 12), adjusted with HCl or NaOH solution (0.1 mol L^{-1}). The pH was measured after 24 h of stirring in an orbital shaker at 150 rpm and 25 °C.
Ash analysis (Muffle, QUIMIS)	Quantify the ash content of the adsorbent materials.	Ash analysis was conducted at 750°C following the Standard Test Method—Designation: D1762-84 (Reapproved in 2021).
Mineral analysis (Milestone microwave digester, model Ethos 1600)	The following metals were quantified: zinc (Zn), Copper (Cu), Manganese (Mn), Potassium (K), Iron (Fe), Sodium (Na), Calcium (Ca), Aluminum (Al), and Magnesium (Mg).	Mineral analysis followed the European Standard EN 15290 (2011).

$$q_t = \frac{(C_o - Ct)\,V}{m} \quad (1)$$

Wherein q_t (mg g^{-1}) is the amount adsorbed on the solid phase at time t; C_o and C_t (mg L^{-1}) are the initial concentration of adsorbate and the concentration of adsorbate at time t, respectively; V (L) is the volume of the solution; and m (g) is the mass of the adsorbent material.

The adsorption isotherm was carried out by adding 50 mL of contaminant solution (acetaminophen or diclofenac) with an initial concentration ranging from 50 to 1000 mg L^{-1} in 20 mg of adsorbent (BT-KOH or Norit), with the equilibrium time obtained in the kinetic tests. The adsorption capacity of BT-KOH and Norit at equilibrium was determined using Eqn (2). The experimental data obtained was fitted to the Langmuir and Freundlich theoretical models, see Table 4.

$$q_e = \frac{(C_0 - C_e)V}{m} \quad (2)$$

Wherein q_e (mg g^{-1}) is the amount of adsorbate adsorbed at equilibrium; C_o and C_e (mg L^{-1}) are the initial concentration of adsorbate and the equilibrium adsorbate concentration, respectively; V (L) is the volume of the solution; and m (g) is the mass of the adsorbent material.

Fixed bed

The continuous system studies were carried out in a jacketed glass column with an internal diameter of 0.5 cm and a height of 5 cm, coupled to a peristaltic pump at the base of the column (upward flow). In all the fixed bed tests, the adsorbent mass was set at 0.2 g, and (inert) sponges supported the bed. The temperature and flow rate were controlled at 25 °C and 3 mL min^{-1}, respectively. Samples of adsorbate were collected at the column outlet at predetermined intervals throughout the experiment to obtain breakthrough curves. The performance of the column was determined by calculating the breakthrough time (t_r, min), the saturation time (t_s, min), the mass transfer zone (MTZ, cm), the volume of effluent that passed through the column up to the saturation point (V_e, mL), the total mass of adsorbate induced in the column up to the saturation point ($m_{adsorbate}$, mg), total mass of adsorbate adsorbed by the adsorbent at the saturation point (m_{total}, mg), and total adsorption capacity in the column (q_{total}, mg g^{-1}) according to Eqns (3)–(9), respectively. The experimental data obtained was adjusted to the theoretical models of Thomas, Adams-Bohart, Yoon-Nelson and Dose–Response.

$$t_r = \frac{C}{C_0} = 0.05 \quad (3)$$

$$t_s = \frac{C}{C_0} = 0.95 \quad (4)$$

$$MTZ = h\left(1 - \frac{t_r}{t_s}\right) \quad (5)$$

$$V_e = Q\,t_s \quad (6)$$

$$m_{adsorbate} = \frac{Q\,C_0\,t_s}{1000} \quad (7)$$

$$m_{total} = \frac{Q C_0}{1000} \int_0^{t_s} \left(1 - \frac{C_{t_s}}{C_0}\right) dt \quad (8)$$

$$q_{total} = \frac{m_{total}}{m_{adsorbent}} \quad (9)$$

Wherein C (mg L^{-1}) is the outlet concentration; C_o (mg L^{-1}) is the inlet concentration; h (cm) is the bed height; m (g) is the adsorbent mass; and Q (L min^{-1}) is the volumetric flow rate.

RESULTS AND DISCUSSION

Characterization of Tingui bark, BT-KOH, and Norit

The nitrogen adsorption/desorption isotherms for Tingui bark, BT-KOH, and Norit are shown in Fig. 1(A)–(C), respectively. Meanwhile, Table 1 shows the values obtained from the nitrogen physisorption analysis. According to the classification established by IUPAC, the N_2 adsorption/desorption isotherm of Tingui bark (Fig. 1(A)) is categorized as Type II. This classification indicates that the adsorbent and adsorbate interactions are comparatively weak and that the adsorbent has a non-porous or macroporous surface.[22] This model aligns with the data provided in Table 1, where Tingui bark exhibited a low BET surface area and a low pore volume.

Moreover, the N_2 adsorption/desorption isotherms exhibited by BT-KOH (Fig. 1(B)) and Norit (Fig. 1(C)) refer to a mixture of type I (b) and IV isotherms. This observation suggests that these materials have wider micropores and narrow mesopores. In addition, their hysteresis pattern is characteristic of narrow slit-shaped pores, a feature often observed in activated carbon materials.[23] Table 2 also shows that the surface area and pore volume of Tingui bark were notably improved through chemical activation with KOH. In chemical activation, the chemical agents develop the porosity through dehydration and degradation of the feedstock structure.[24] Activation with KOH occurs by collapsing the carbon network by transforming KOH into K_2CO_3. The gaseous species of CO, CO_2, H_2O, and H_2 generated during activation leave the material, generating pores, whereas the metallic K generated *in situ* diffuses into the internal structure.[25] Also, the removal of potassium salts and metallic K by washing creates the microporosity.[24]

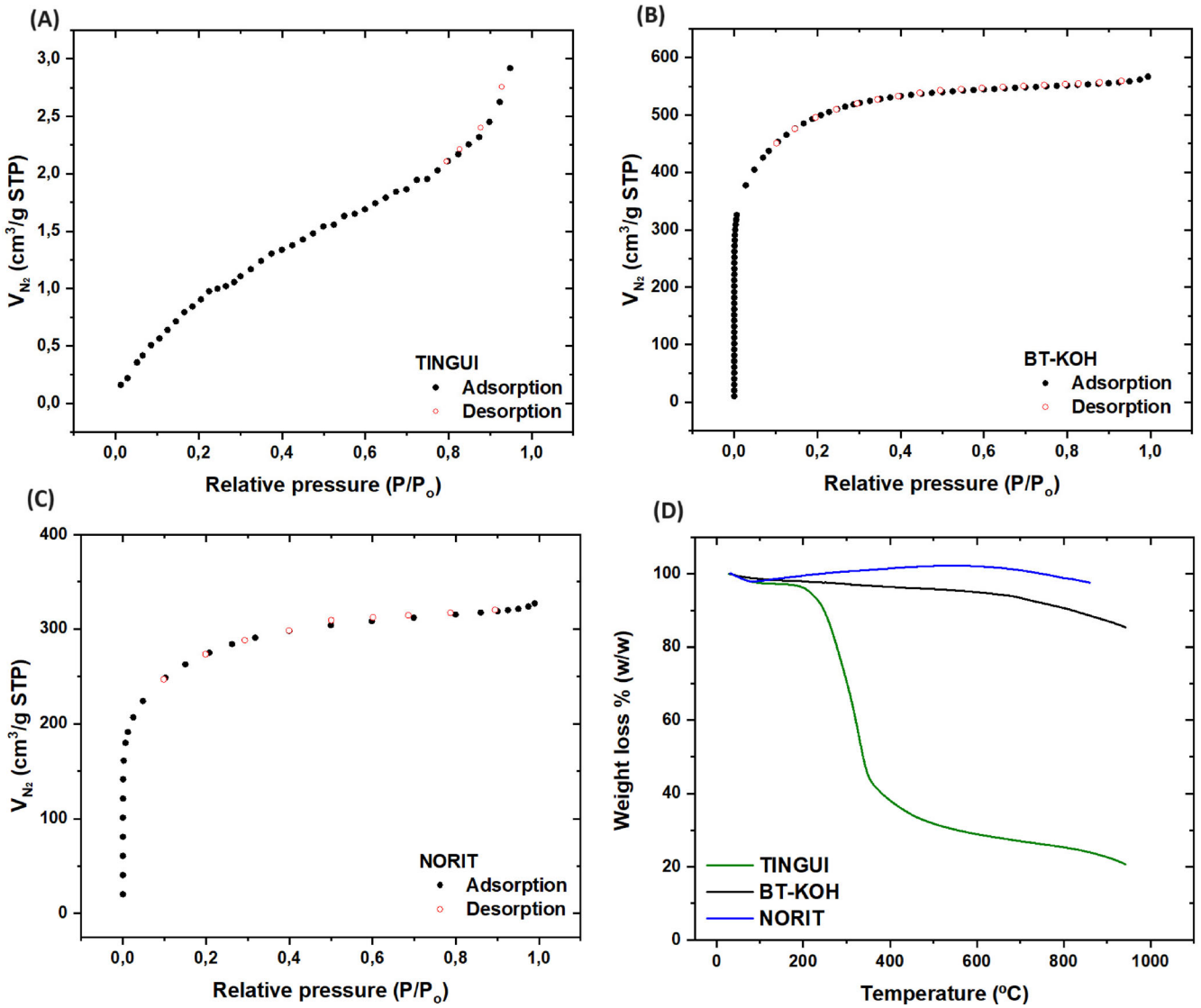

Figure 1. N_2 adsorption/desorption isotherms of Tingui (A), TB-KOH (B) and Norit (C). TGA analysis of Tingui, BT-KOH and Norit (D).

Table 2. Material characteristics

Characteristics	Tingui	BT-KOH	Norit
Nitrogen adsorption			
S_{BET} ($m^2\ g^{-1}$)	4.033	1775	966
D_P (nm)	6.38	1.97	2.06
V_P ($cm^3\ g^{-1}$)	6.43×10^{-3}	0.873	0.497
V_{microp} ($cm^3\ g^{-1}$)	0.00	0.374	0.360
V_{mesop} ($cm^3\ g^{-1}$)	6.43×10^{-3}	0.499	0.137
Elemental analysis			
C (%)	47.41	72.86	80.1
H (%)	5.77	0.36	0.3
N (%)	1.46	0.39	0.4
S (%)	<0.03	<0.03	<0.03
O (%)[a]	45.36	26.39	19.2
Zero charge point analysis			
pH_{PCZ}	nd	5.91	8.00
Analysis of ash (%) and metals (mg g^{-1})			
Ash	2.18	1.73	11.60
Al	0.0251	0.0650	13.47
Ca	0.534	0.208	1.52
Cu	<0.001	<0.001	0.009
Fe	0.066	0.705	7.26
K	5.417	1.444	0.623
Mg	0.498	0.189	0.170
Mn	0.008	0.010	0.030
Na	<0.0002	<0.0002	0.257
Zn	<0.0004	<0.0004	0.020

[a] By difference; nd, not determined.

Furthermore, in the data presented in Table 2, BT-KOH shows a higher S_{BET} and V_P than Norit. An adsorbent with higher S_{BET} and V_P exhibits a remarkable capacity for adsorbing aromatic pollutants, especially if pore filling is the primary adsorption mechanism.[26] Therefore, it is expected that BT-KOH, with its higher specific surface area and well-developed internal pore structure, can efficiently remove acetaminophen and diclofenac molecules from the aquatic environment through the pore-filling mechanism.

Regarding the thermal stability of activated carbon, TGA analysis (as shown in Fig. 1(D)) revealed that Tingui bark showed three distinct stages of mass loss. The initial phase, responsible for a mass loss of 3.4%, occurred between 50 and 200 °C, indicating the removal of physically adsorbed water through dehydration.[27] The subsequent mass loss, totaling 69.6%, occurred in the 200 to 700 °C temperature range. This significant loss can be attributed to the decomposition of lignocellulosic components, such as cellulose, hemicellulose, and lignin, present in the biomass.[28] The final mass loss of 6.3% occurred in the 700 to 950 °C temperature range. This loss is attributed to the sample's decomposition of residual lignin and carbonaceous materials.[29] BT-KOH and Norit showed remarkable stability about the activated carbons, with mass losses of 10.04% and 2.42% at 800 °C, respectively.

The data obtained from the elemental analysis is shown in Table 2. Compared to Norit, BT-KOH had a lower carbon and oxygen content. These results indicate that the surface of BT-KOH has more oxygen than that of Norit. This suggests that BT-KOH may have more hydroxyl functional groups (—OH) than Norit, which favors the adsorption of organic contaminants. This is because the presence of hydroxyl groups increases the polarity of the surface of the adsorbent material, which can improve its affinity with various substances.[30]

The point of zero charge (PZC) is an important parameter that describes the pH at which an adsorbent material's surface has a zero net charge. In other words, it is the point at which the amount of positive and negative charges on the material's surface equalizes. For BT-KOH and Norit, these values were determined as 5.91 and 8.0, respectively, as detailed in Table 2. These results reveal significant differences, such as the surface difference between these adsorbent materials. BT-KOH has a relatively low PZC, indicating a tendency towards an acidic surface, while Norit has a higher PZC, suggesting a basic surface nature.[31] These characteristics have important implications for the adsorption of compounds in solution, especially about their isoelectric points (pH at which the net charge of the molecule is zero). For example, the material's surface will be predominantly positively charged in a medium with a pH below the PZC of BT-KOH. In contrast, in a medium with a pH above the PZC of Norit, the surface will be predominantly negatively charged.[8]

The ash and metal content results are also shown in Table 2. It can be seen that Norit has the highest levels of these elements compared to BT-KOH. This significant difference could considerably impact the adsorption efficiency of the adsorbents. A more substantial amount of ash and inorganic matter in an adsorbent can significantly compromise its adsorption efficiency. These unwanted materials can interfere with the active sites available for adsorption, competing with the target contaminants and thus reducing the removal capacity. The ash in the adsorbent can clog the pores, reducing the surface area available for interacting with the contaminants. This limits the adsorbent's ability to efficiently capture unwanted molecules, reducing the effectiveness of the adsorption process. In addition, metals can trigger undesirable reactions with contaminants or interfere with forming adsorbent-contaminant complexes, thus impairing removal capacity. These metals can act as catalysts for chemical reactions that reduce the affinity of the adsorbent for the contaminant or lead to the formation of unwanted products.

The FTIR analysis technique provides a qualitative view of the functional groups on the surface of adsorbent materials. These groups play a fundamental role in the adsorption capacity of adsorbates in aqueous solutions.[32] The FTIR spectra of the materials are shown in Fig. 2. As can be seen, Norit and BT-KOH showed similar spectra. The FTIR revealed the presence of chemical groups on the surface of both adsorbents, as evidenced by the broad peaks at 3600 and 3410 cm^{-1} (A and B) associated with the elongation of the —OH group. The band at 2960 cm^{-1} (C) is attributable to the stretching vibrations of the C—H groups.[33] The peak at 2300 cm^{-1} (D) is attributed to the —OH stretching of the carboxylic acid.[34] The band at 1780 cm^{-1} (E) can be attributed to the symmetrical stretching of the C═O group referring to the carboxylic acid portions.[35] The band at 1610 cm^{-1} (F) is characteristic of stretching the C—O double bond in esters or carboxylic acids. The small peaks at 1390 cm^{-1} (G) are attributed to the ring modes of aromatic compounds. The peaks at 1030 and 1000 cm^{-1} (H and I) are associated with the C—O stretching of phenolic or carboxylate groups.[36] The peaks at 800, 600, and 450 cm^{-1} (J, K, and L) are associated with stretching vibrations of the C—N or C—O group.[37] It is also observed that, in the FTIR of Tingui, the peaks at 1030 and 1000 cm^{-1} (designated as H and I) correspond to the C—O stretching of phenolic and/or carboxylate functional groups present on the surface. However,

these peaks are significantly reduced in the BT-KOH spectrum, which indicates the removal of these groups during the KOH activation process. This removal occurs due to the caustic effect of KOH, which favors the degradation and volatilization of these oxygenated groups. This process contributes to the increase in the surface area and porosity of the activated material, since the elimination of the oxygenated groups expands the pores and improves the microporous structure of BT-KOH.[38]

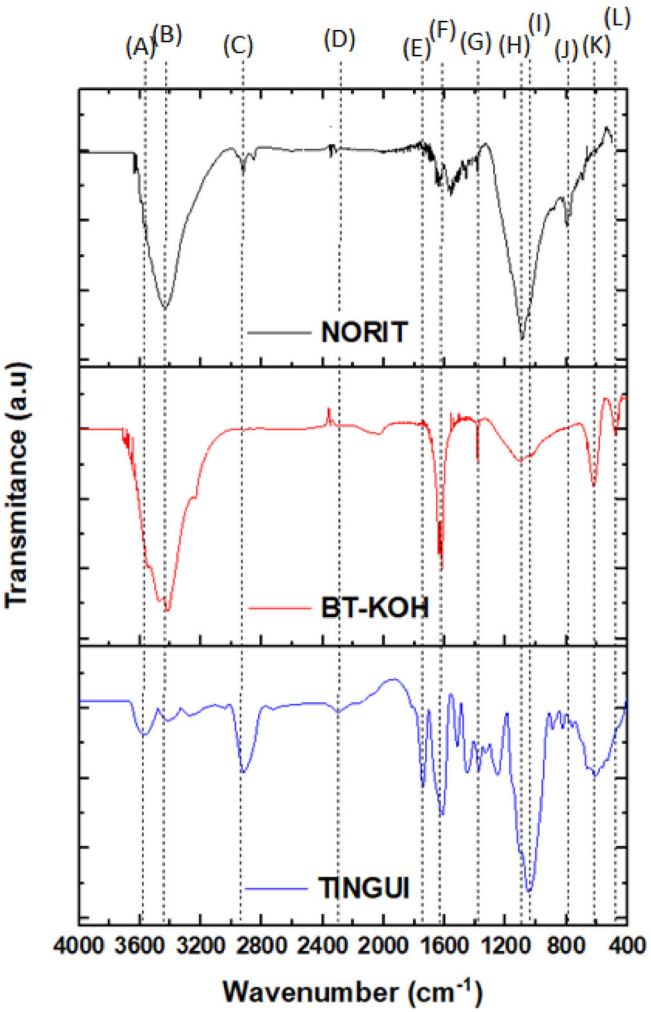

Figure 2. FTIR of Tingui biomass, BT-KOH, and Norit.

Tingui bark SEM image (Fig. 3(A)) showed heterogeneous characteristics structure in the form of cracks, roughness, and crevices. Ordered fibrils are also seen, in consonance with a lignocellulosic structure. After activation, BT-KOH (Fig. 3(B)) changed to a completely different morphology. It is possible to observe a larger number of cavities, smaller in diameter, indicating the development of pores. In fact, KOH activation generally promotes disruption of the raw material. Thus, no morphological similarities to the raw material are observed.[39]

Adsorption kinetic

Figure 4(A), (B) show the adsorption kinetics of Norit and BT-KOH for acetaminophen and diclofenac, respectively. The Pseudo-First Order (PFO), Pseudo-Second Order (PSO), and Elovich theoretical models were selected to describe the experimental data, as detailed in Table 3.

The time required to reach equilibrium in the removal of acetaminophen by both Norit and BT-KOH was 540 min, whereas, for diclofenac, this time was 1440 min. These values represent the period in which the adsorption rate stabilizes, indicating that the amount of acetaminophen or diclofenac adsorbed by the adsorbents does not increase significantly after this point.[40] This equilibrium time is essential to understand adsorption efficiency and determine the time required for water treatment or environmental remediation.[41]

This discrepancy in equilibrium time suggests that removing diclofenac takes longer than removing acetaminophen when using Norit and BT-KOH as adsorbents. One reason for this difference in equilibrium time between acetaminophen and diclofenac lies in the competition for new active sites. Different compounds can interact in other ways with adsorbents, competing for the sites available for adsorption. Thus, the increase in contact time required for diclofenac can be attributed, in part, to this greater competition for active adsorption sites.[42]

At the equilibrium point, it was also observed that Norit removed 145.9 mg g^{-1} of acetaminophen, while BT-KOH removed 191.4 mg g^{-1}. The Pseudo-Second-Order was the theoretical model that best described the experimental data for acetaminophen adsorption. Norit removed 133.3 mg g^{-1} from diclofenac, while BT-KOH removed 157.4 mg g^{-1}. The theoretical model that best described the experimental data for diclofenac adsorption was that of Elovich.

The choice of kinetic models was crucial to interpreting the experimental data. The Pseudo-Second-Order model adopted for acetaminophen is based on the premise that the adsorption rate is controlled by the speed of adsorption on the solid surface.

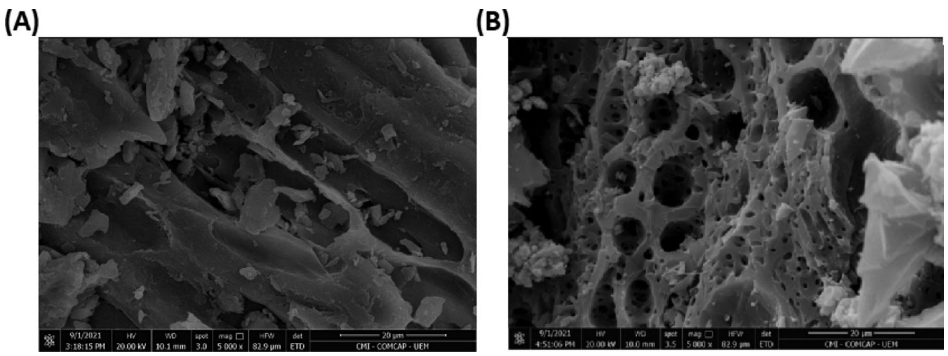

Figure 3. SEM images of Tingui bark in 5000× (A), BT-KOH in 5000× (B)

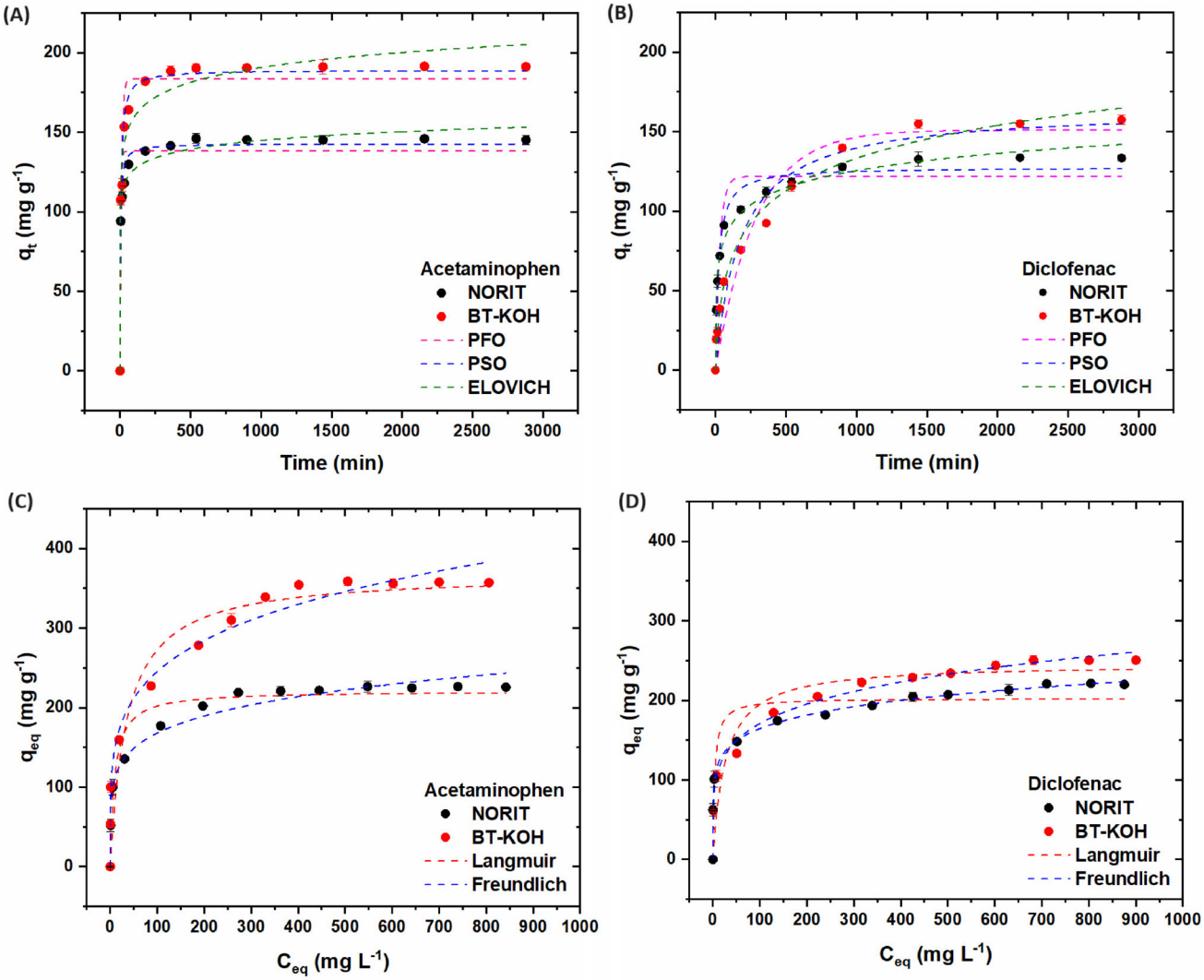

Figure 4. Adsorption kinetics of acetaminophen (A) and diclofenac (B) by Norit and BT-KOH. Adsorption isotherm of acetaminophen (C) and diclofenac (D) by Norit and BT-KOH.

Table 3. Adsorption kinetic parameters of Norit and BT-KOH

		Acetaminophen		Diclofenac	
Model	Parameters	Norit	BT-KOH	Norit	BT-KOH
PFO	q_e (mg g^{-1})	138.1	183.7	121.73	150.98
$q_t = q_e(1-e^{-K_1 t})$	k_1 (min^{-1})	0.186	0.0943	0.0324	0.0035
	R^2	0.935	0.917	0.922	0.936
PSO	q_e (mg g^{-1})	142.7	189.1	127.6	162.6
$q_t = \frac{K_2 q_e^2 t}{1+K_2 q_e t}$	k_2 (min^{-1})	2.06×10^{-3}	9.00×10^{-3}	3.70×10^{-4}	3.70×10^{-5}
	R^2	0.983	0.980	0.970	0.965
Elovich	α (mg g^{-1} min^{-1})	7.29×10^{6}	1.78×10^{4}	49.54	2.48
$q_t = \frac{1}{\beta}\ln(1+\alpha\beta t)$	β (mg g^{-1})	0.126	0.0739	0.0643	0.0332
	R^2	0.982	0.962	0.990	0.990

Nevertheless, the Elovich model, selected for diclofenac, describes the adsorption kinetics considering the gradual filling of the available adsorption sites on the solid surface over time.

Furthermore, these results suggest that BT-KOH has a higher adsorption capacity for acetaminophen and diclofenac than Norit. This difference may be related to the specific physicochemical

properties of each adsorbent, such as surface area and functional groups available for interaction with the adsorbed molecules.[43]

Another explanation for BT-KOH having a greater adsorption capacity than Norit is correlated with the type of nitrogen adsorption/desorption isotherms of each material. Type I isotherms (BT-KOH) are characteristic of microporous adsorbents, which exhibit strong adsorption at low pressures and saturation at high pressures. This suggests that the material has a highly developed porous structure with many micropores, allowing a higher adsorption capacity for small molecules. Type IV (Norit) isotherms are associated with mesoporous adsorbents and may present different adsorption behavior, such as increased adsorption at moderate pressures and saturation behavior at higher pressures, although less pronounced than in Type I isotherms.[44] Thus, BT-KOH, with its micropore structure, may also have a faster adsorption rate, as the molecules have more adsorption sites available from the beginning of the adsorption process, whereas Norit may have a slower or less efficient adsorption rate for certain contaminants, due to the need for the molecules to move into the mesopores, which may take longer.

These findings contribute to a more complete understanding of the adsorption kinetics of these drugs by different adsorbents, providing essential insights for practical applications in pollutant removal and treatment processes.

Adsorption isotherm

Figure 4(C), (D) show the adsorption isotherms of Norit and BT-KOH for acetaminophen and diclofenac, respectively. In this analysis, the Langmuir and Freundlich theoretical models were selected to describe the experimental data, as detailed in Table 4.

The maximum adsorption capacity of Norit and BT-KOH to remove acetaminophen was 226.3 and 357.7 mg g^{-1}, respectively. For diclofenac, these values were 220.9 and 250.6 mg g^{-1}, respectively. It can be seen that BT-KOH had a higher adsorption capacity for both contaminants compared to Norit, as was also observed in the experimental adsorption kinetics data.

This significant discrepancy in adsorption capacity between the two adsorbent materials can be explained by several different characteristics, such as chemical composition, surface area, porosity, and the presence of functional groups on the surface of the materials, as evidenced by the results of the physicochemical analyses of each adsorbent. As revealed by these analyses, BT-KOH had more oxygen-containing functional groups and higher S_{BET} than Norit. Due to its greater adsorption capacity, BT-KOH is potentially more efficient at removing acetaminophen and diclofenac from the solution, making it a more promising candidate for water treatment and environmental remediation applications. Furthermore, Table 5 presents the maximum adsorption capacity of different adsorbent materials. The results also demonstrate that

Table 4. Parameters of the BT-KOH and Norit adsorption isotherm

Model	Parameters	Acetaminophen		Diclofenac	
		Norit	BT-KOH	Norit	BT-KOH
Langmuir	q_{max} (mg g^{-1})	220.8	368.3	202.57	245.99
$q_e = \frac{q_{max} K_L C_e}{1 + K_L C_e}$	k_L (L mg^{-1})	0.106	0.0284	0.263	0.0382
	R^2	0.947	0.927	0.865	0.903
	SSR	333.6	1342.9	713.86	706.82
Freundlich	k_F (mg g^{-1})/(L mg^{-1})$^{1/n}$	75.23	91.60	85.91	70.42
$q_e = K_F C_e^{\frac{1}{n}}$	n	5.73	4.70	7.09	5.20
	R^2	0.980	0.990	0.932	0.992
	SSR	154.12	250.60	361.9	51.80

Table 5. Maximum adsorption capacities of acetaminophen and diclofenac on different adsorbents

Adsorbent	Experimental conditions				Contaminant	$q_{máx}$ (mg g^{-1})	Reference
	T (°C)	Mass (mg)	Time (min)	$C_{initial}$ (mg L^{-1})			
Banana peel	45	2000	1500	0–200	Acetaminophen	57.3	51
Calcium alginate/activated hydrochar composite	25	25	240	25–1000	Acetaminophen	165.94	27
Brazil nutshells	45	30	10	100–1500	Acetaminophen	232.6	32
Guazuma ulmifolia Lam. fruit	45	25	1440	20–350	Diclofenac	27.80	14
Apricot seeds activated carbon	25	267	150	30	Diclofenac	5.35	15
Palm fibers functionalized with FAH_2O_2	25	250	150	0–120	Diclofenac	33.12	13
BT-KOH	25	20	540	50–1000	Acetaminophen	357.7	This work
BT-KOH	25	20	1440	50–1000	Diclofenac	250.6	This work
Norit	25	20	540	50–1000	Acetaminophen	226.3	This work
Norit	25	20	1440	50–1000	Diclofenac	220.9	This work

BT-KOH stands out among other adsorbents, evidencing its effectiveness in the removal of diclofenac and acetaminophen. This also indicates that BT-KOH is a promising alternative for the treatment of contaminated water.

Furthermore, the Freundlich model best fits the experimental data for substances and adsorbent materials. This suggests that the adsorption of the contaminants does not strictly follow the monolayer behavior proposed by the Langmuir model but rather a multilayer adsorption process, where the amount adsorbed increases proportionally to the concentration of the contaminant in the solution.[45] Thus, the multi-surface adsorption observed may have unfolded in two distinct phases, the first on the available surface adsorption sites, followed by interactions between the adsorbed molecules.[46]

The parameter *n* in the Freundlich equation plays a fundamental role in characterizing the reactivity and heterogeneity of an adsorbent's active sites. A value of *n* greater than 1 implies that the adsorption process is predominantly chemical, indicating a considerable affinity of the contaminants for the adsorption sites. In this work, the value of *n* for all the situations investigated was more significant than 1, pointing to a high affinity of acetaminophen and diclofenac for the adsorption sites in the adsorbent materials. This finding suggests a strong interaction between the contaminants and the adsorbents and significant binding energy, highlighting the effectiveness of these materials in removing these unwanted compounds.[8]

Fixed bed

Figure 5(A), (B) present the studies obtained on the adsorption of acetaminophen and diclofenac by Norit and BT-KOH in a fixed-bed column, respectively. Furthermore, column performance data regarding acetaminophen and diclofenac removal are presented in Tables 6 and 7, respectively.

Comparing the results obtained in the adsorption of acetaminophen and diclofenac by BT-KOH and Norit in a fixed bed (see Tables 6 and 7), it was possible to observe that, although both experiments used the same initial conditions in terms of adsorbent mass, flow rate and initial contaminant concentration, BT-KOH showed longer retention and saturation times as well as a higher maximum adsorption capacity and a higher removal efficiency compared to Norit for the two contaminants tested. This can be attributed to the height of the adsorbent bed, where as the bed increases, the contact time of the solute present in the solution with the compacted bed increases. Thus, interparticle diffusion in the pores is improved.[27] These results suggest that BT-KOH is more effective in removing acetaminophen and diclofenac in fixed bed systems, making it a preferred choice for water treatment applications contaminated by these pharmaceutical contaminants.

The theoretical dose–response model was the one that best fitted the experimental data on acetaminophen or diclofenac adsorption, both for BT-KOH and Norit. Its relevance lies in the fact that it describes the complete rupture curve with high precision, in addition to being able to reduce errors associated with the use of the Thomas model, especially at low or high removal times.[9] Furthermore, in the adsorption of contaminants by adsorbent materials, the dose–response model is applied to quantify the relationship between the concentration of the contaminant in the solution and the amount adsorbed by the adsorbent. Specifically, the model describes how the adsorption capacity of the material varies in response to the concentration of the contaminant in the solution.

Possible adsorption mechanism

The adsorption of acetaminophen and diclofenac on carbonaceous adsorbents is a complex process influenced by various macroscopic and microscopic interactions. The pharmaceutical compounds' unique properties determine their affinity and adsorption behavior on carbonaceous surfaces. The interactions involved in this process are diverse and include hydrogen bonds, π-π interactions, n-π interactions, and pore filling. These mechanisms play distinct roles in the adsorption of these drugs and are influenced by factors such as the chemical structure of the compounds, the morphology of the adsorbent, discussed in SEM analysis, and the environmental conditions.[26,47,48]

Hydrogen bonds can be established in two different ways. Firstly, dipole–dipole H bonds occur between the surface hydrogen of the hydroxyl groups (—OH) present on the surface of the

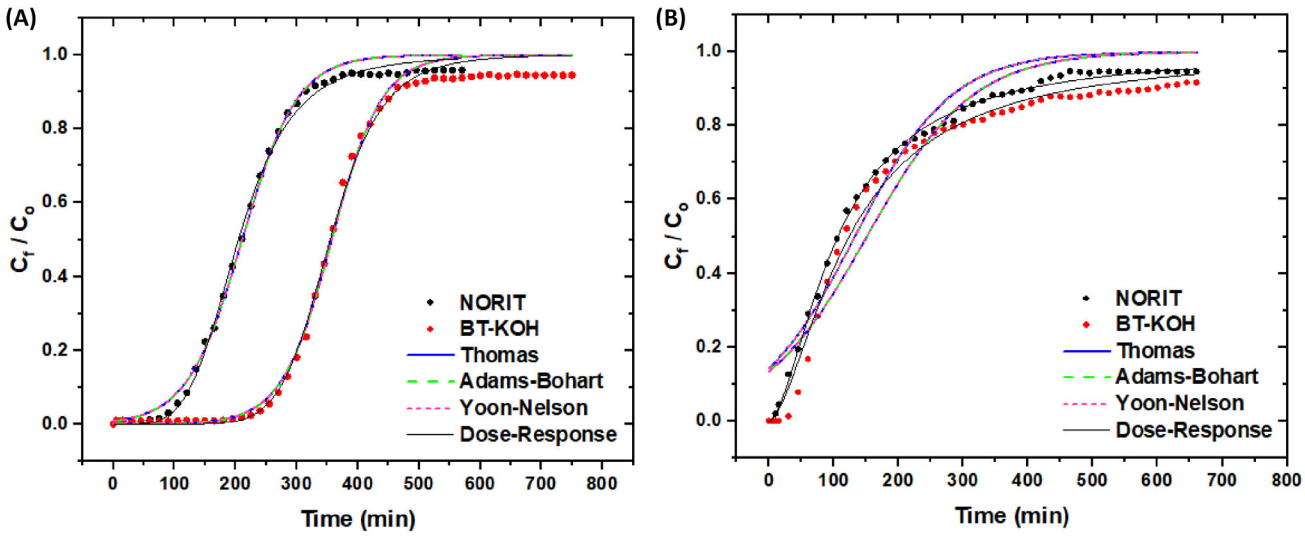

Figure 5. Breakthrough curves with mathematical modeling of acetaminophen (A) and diclofenac (B) adsorption on Norit and BT-KOH.

Table 6. Parameters of the Thomas, Adams-Bohart, Yoon-Nelson, Dose–Response model using Norit and BT-KOH to remove acetaminophen (50 mg L^{-1})

Model	Parameters	Norit	BT-KOH
		m = 0.2 g Q = 3 mL min^{-1} Co = 50 mg L^{-1} Z = 1.4 cm t_r (C_t/C_0 = 0.05) = 101.1 min t_s (C_t/C_0 = 0.94) = 387.1 min ZTM = 1.03 cm V_{eflu} = 1161.42 mL m_{DIC_total} = 58.07 mg m_{DIC_ads} = 32.31 mg q_{total} = 161.6 mg g^{-1} %R = 55.65%	m = 0.2 g Q = 3 mL min^{-1} Co = 50 mg L^{-1} Z = 2.2 cm t_r (C_t/C_0 = 0.05) = 250.6 min t_s (C_t/C_0 = 0.94) = 578.3 min ZTM = 1.24 cm V_{eflu} = 1734.8 mL m_{DIC_total} = 86.7 mg m_{DIC_ads} = 53.7 mg q_{total} = 268.3 mg g^{-1} %R = 61.85%
Thomas $\frac{C}{C_0}=\frac{1}{1+\exp\left[\left(\frac{K_{TH}}{Q}\right)(q_0 m - C_0 Qt)\right]}$	k_{Th} (L mg^{-1} min^{-1}) q_o (mg g^{-1}) R^2	4.46×10^{-3} 7.90 0.995	4.87×10^{-3} 13.39 0.994
Adams-Bohart $\frac{C}{C_0}=\frac{\exp(K_{AB}C_0 t)}{\exp\left(\frac{K_{AB}N_0 h}{v}\right)-1+\exp(K_{AB}C_0 t)}$	k_{AB} (L mg^{-1} min^{-1}) N_o (mg L^{-1}) R^2	4.46×10^{-3} 8068.5 0.995	4.87×10^{-3} 13 646.0 0.994
Yoon-Nelson $\frac{C}{C_0}=\frac{1}{1+\exp[k_{YN}(\tau - t)]}$	k_{YN} (min^{-1}) τ_{cal} (min) R^2	0.0223 210.7 0.995	0.0242 375.1 0.994
Dose–Response $\frac{C}{C_0}=1-\frac{1}{1+\left(\frac{C_0 Qt}{q_0 m}\right)^{\alpha}}$	α q_o (mg g^{-1}) R^2	4.51 7.68 0.998	8.35 13.30 0.996

Table 7. Parameters of the Thomas, Adams-Bohart, Yoon-Nelson, Dose–Response model using Norit and BT-KOH to remove diclofenac (50 mg L^{-1})

Model	Parameters	Norit	BT-KOH
		m = 0.2 g Q = 3 mL min^{-1} Co = 50 mg L^{-1} Z = 1.4 cm t_r (C_t/C_0 = 0.05) = 15.9 min t_s (C_t/C_0 = 0.94) = 456.1 min ZTM = 1.35 cm V_{eflu} = 1368.3 mL m_{DIC_total} = 68.4 mg m_{DIC_ads} = 22.2 mg q_{total} = 110.9 mg g^{-1} %R = 32.42%	m = 0.2 g Q = 3 mL min^{-1} Co = 50 mg L^{-1} Z = 2.2 cm t_r (C_t/C_0 = 0.05) = 38.6 min t_s (C_t/C_0 = 0.94) = 756.2 min ZTM = 2.1 cm V_{eflu} = 2268.4 mL m_{DIC_total} = 113.4 mg m_{DIC_ads} = 29.3 mg q_{total} = 146.6 mg g^{-1} %R = 35.85%
Thomas $\frac{C}{C_0}=\frac{1}{1+\exp\left[\left(\frac{K_{TH}}{Q}\right)(q_0 m - C_0 Qt)\right]}$	k_{Th} (L mg^{-1} min^{-1}) q_o (mg g^{-1}) R^2	2.80×10^{-4} 95.96 0.945	2.6×10^{-4} 109.31 0.895
Adams-Bohart $\frac{C}{C_0}=\frac{\exp(K_{AB}C_0 t)}{\exp\left(\frac{K_{AB}N_0 h}{v}\right)-1+\exp(K_{AB}C_0 t)}$	k_{AB} (L mg^{-1} min^{-1}) N_o (mg L^{-1}) R^2	2.70×10^{-4} 108.4×10^{3} 0.945	2.50×10^{-4} 77.9×10^{3} 0.895
Yoon-Nelson $\frac{C}{C_0}=\frac{1}{1+\exp[k_{YN}(\tau - t)]}$	k_{YN} (min^{-1}) τ_{cal} (min) R^2	0.0135 132.8 0.945	0.0123 151.16 0.896
Dose–Response $\frac{C}{C_0}=1-\frac{1}{1+\left(\frac{C_0 Qt}{q_0 m}\right)^{\alpha}}$	α q_o (mg g^{-1}) R^2	1.66 78.62 0.998	1.63 91.44 0.991

adsorbent and appropriate atoms, such as oxygen and nitrogen, in the aromatic molecules of the adsorbate. Secondly, there is the Yoshida H bond between the aromatic ring in the adsorbate molecules and the hydroxyl groups (—OH) on the surface of the adsorbent. In the case of acetaminophen, the oxygen and nitrogen atoms in its structure play the role of hydrogen receptors, while the —OH groups on the adsorbent surface act as hydrogen donors.[43] As for diclofenac, the amino and carboxyl groups present in its molecule form hydrogen bonds with the oxygen-containing functional groups on the surface of the adsorbent material.[49]

The π-π interaction occurs when the aromatic rings of the drug molecules approach and interact with the aromatic structure of the carbonaceous adsorbents. Acetaminophen's molecule's —OH and —NH groups act as influential electron donors.[44] Diclofenac's rich density of π electrons and the benzene rings' delocalization characteristics in its molecule favor the generation of π-π interactions.[50]

On the other hand, the n-π interaction occurs when electron-depleted sites on the adsorbate molecules and π-electron donors, such as oxygen electron pairs, form a donor-acceptor complex. In this case, the aromatic rings of the acetaminophen and diclofenac molecules serve as electron acceptors, while the oxygen groups on the adsorbent surface, such as —COOH and —OH, act as electron donors.[26]

Finally, pore filling is considered the dominant adsorption mechanism for acetaminophen and diclofenac on carbonaceous adsorbents. The drug molecules are adsorbed in the pores of the carbonaceous structure, which provides a large surface area for the interaction between the drug molecules and the adsorbent.[43]

Together, these interaction mechanisms contribute to the complexity of the acetaminophen and diclofenac adsorption process on carbonaceous adsorbents. Understanding these mechanisms is essential for developing effective environmental remediation strategies and optimizing controlled drug release systems based on carbonaceous materials.

CONCLUSION

It is concluded that the adsorbent developed from Tingui bark and activated with KOH (BT-KOH) showed superior performance in removing acetaminophen and diclofenac, both in terms of batch and fixed bed adsorption, when compared to the commercial adsorbent (Norit).

The superiority of BT-KOH is attributed to its distinct physicochemical characteristics. Its more developed surface and higher oxygen content provide a more effective adsorption capacity for organic contaminants present in water. These results offer encouraging prospects for the practical application of this adsorbent in environmental remediation and contaminated water treatment processes.

Using materials of natural origin, such as Tingui bark, demonstrates a sustainable approach to developing environmental technologies. This innovation demonstrates efficiency and reduces environmental impact by taking advantage of renewable resources and avoiding the waste of agricultural residues.

However, despite the promising results, it is essential to highlight the need for further research. Fully understanding the mechanisms underlying the adsorption process and further optimizing the efficiency of BT-KOH are crucial steps to ensure its viability and widespread application.

In short, the development of the BT-KOH adsorbent represents a significant advance in removing organic contaminants from water. Its superior efficacy and sustainable origin offer a promising solution to pressing environmental challenges, indicating a positive path toward protecting and preserving water resources.

ACKNOWLEDGEMENTS

This study was funded in part by the National Council for Scientific and Technological Development—CNPq (Process 170734/2023-4). This work was also funded by the Associate Laboratory for Green Chemistry—LAQV which is financed by national funds from FCT/MCTES (UIDB/50006/2020 DOI 10.54499/UIDP/50006/2020).

AUTHOR CONTRIBUTION

Débora Federici dos Santos—Methodology, Investigation, Writing—Original Draft.

Wardleison Martins Moreira—Methodology, Investigation, Writing—Original Draft.

Thiago Peixoto de Araújo—Data curation, Writing—Original Draft.

Maria Manuel Serrano Bernardo—Investigation, Writing—Review & Editing.

Isabel Maria de Figueiredo Ligeiro da Fonseca—Writing—Review & Editing.

Indianara Conceição Ostroski—Resources, Writing—Review & Editing, Supervision.

Maria Angélica Simões Dornellas de Barros—Resources, Writing—Review & Editing, Supervision, Project administration.

Eduardo Falabella Sousa-Aguiar—Resources, Writing—Review & Editing, Supervision, Project administration.

All authors read and approved the final manuscript.

DATA AVAILABILITY STATEMENT

Some or all data, models, or code that support the findings of this study are available from the corresponding author upon reasonable request.

ETHICS STATEMENT

We assure that this manuscript is original work and this work was neither accepted nor submitted simultaneously to any other journals.

CONFLICT OF INTEREST

The authors declare that they have no competing interests.

REFERENCES

1 Jimenez-López BA, Leyva-Ramos R, Mendoza-Mendoza E, Villela-Martínez DE and Carrales-Alvarado DH, Adsorption of diclofenac from water solution on layered double hydroxide Mg/Al/CO3 synthesized from sulphate salts and calcined. *Environ Nanotechnol, Monit. Manage* **20**:100782 (2023). https://doi.org/10.1016/j.enmm.2023.100782.

2 Gómez-Avilés A, Sellaoui L, Badawi M, Bonilla-Petriciolet A, Bedia J and Belver C, Simultaneous adsorption of acetaminophen, diclofenac and tetracycline by organo-sepiolite: experiments and statistical physics modelling. *Chem Eng J* **404**:126601 (2021). https://doi.org/10.1016/j.cej.2020.126601.

3 Ntone EPN, Rahman SA, Samah RA, Wahab MSA, Jawad ZA and Hasbullah H, A comparison study on performance of thin film

composite membrane embedded with graphene oxide for acetaminophen, diclofenac and ibuprofen separation from waste water. *Chem Eng Res Des* **195**:28–37 (2023). https://doi.org/10.1016/j.cherd.2023.05.023.
4 Ortiz-bustos J, Soares SF, Helena P and Yolanda P, Tuning adsorption capacities of hybrid mesoporous silica nanospheres and adsorption mechanism study for sulfamethoxazole and diclofenac removal from water. *J Mol Liq* **398**:124213 (2024). https://doi.org/10.1016/j.molliq.2024.124213.
5 Gavrilescu M, Demnerová K, Aamand J, Agathos S and Fava F, Emerging pollutants in the environment: present and future challenges in biomonitoring, ecological risks and bioremediation. *New Biotechnol* **32**:147–156 (2015). https://doi.org/10.1016/j.nbt.2014.01.001.
6 de Oliveira M, Frihling BEF, Velasques J, Filho FJCM, Cavalheri PS and Migliolo L, Pharmaceuticals residues and xenobiotics contaminants: occurrence, analytical techniques and sustainable alternatives for wastewater treatment. *Sci Total Environ* **705**:135568 (2020). https://doi.org/10.1016/j.scitotenv.2019.135568.
7 Lai LW, Teh LP, Timmiati SN, Kamarudin NHN and Setiabudi HD, A sustainable solution for diclofenac adsorption: chitosan-modified fibrous silica KCC-1 adsorbent. *J Environ Chem Eng* **11**:111295 (2023). https://doi.org/10.1016/j.jece.2023.111295.
8 Mokhtaryan S, Khodabakhshi A, Sadeghi R, Nourmoradi H, Shakeri K, Hemati S *et al*., New activated carbon derived from Gundelia tournefortii seeds for effective removal of acetaminophen from aqueous solutions: adsorption performance. *Arab J Chem* **16**:105253 (2023). https://doi.org/10.1016/j.arabjc.2023.105253.
9 Vera M, Juela DM, Cruzat C and Vanegas E, Modeling and computational fluid dynamic simulation of acetaminophen adsorption using sugarcane bagasse. *J Environ Chem Eng* **9**:105056 (2021). https://doi.org/10.1016/j.jece.2021.105056.
10 dos Reis GS, Guy M, Mathieu M, Jebrane M, Lima EC, Thyrel M *et al*., A comparative study of chemical treatment by MgCl2, ZnSO4, ZnCl2, and KOH on physicochemical properties and acetaminophen adsorption performance of biobased porous materials from tree bark residues. *Colloids Surf, A* **642**:128626 (2022). https://doi.org/10.1016/j.colsurfa.2022.128626.
11 Mukherjee T and Rahaman M, Optimization of acetaminophen adsorption onto biodegradable waste-derived activated carbon using response surface methodology. *Mater Today Proc* **76**:233–238 (2023). https://doi.org/10.1016/j.matpr.2023.01.051.
12 Yanyan L, Kurniawan TA, Zhu M, Ouyang T, Avtar R, Dzarfan Othman MH *et al*., Removal of acetaminophen from synthetic wastewater in a fixed-bed column adsorption using low-cost coconut shell waste pretreated with NaOH, HNO3, ozone, and/or chitosan. *J Environ Manage* **226**:365–376 (2018). https://doi.org/10.1016/j.jenvman.2018.08.032.
13 Darryle CM, Acayanka E, Takam B, Line LN, Kamgang GY, Laminsi S *et al*., Influence of plasma-based surface functionalization of palm fibers on the adsorption of diclofenac from water: experiments, thermodynamics and removal mechanism. *J Water Process Eng* **43**:102254 (2021). https://doi.org/10.1016/j.jwpe.2021.102254.
14 Araujo LA, Bezerra CO, Cusioli LF, Rodríguez MT, Gomes RG and Bergamasco R, Diclofenac adsorption using a low-cost adsorbent derived from Guazuma ulmifolia lam. Fruit via chemical and thermal treatment. *J Environ Chem Eng* **9**:106629 (2021). https://doi.org/10.1016/j.jece.2021.106629.
15 Salman SD, Rasheed IM and Ismaeel MM, Removal of diclofenac from aqueous solution on apricot seeds activated carbon synthesized by pyro carbonic acid microwave. *Chem Data Collect* **43**:100982 (2023). https://doi.org/10.1016/j.cdc.2022.100982.
16 Prauchner MJ and Rodríguez-Reinoso F, Chemical versus physical activation of coconut shell: a comparative study. *Microporous Mesoporous Mater* **152**:163–171 (2012). https://doi.org/10.1016/j.micromeso.2011.11.040.
17 Maciá-Agulló JA, Moore BC, Cazorla-Amorós D and Linares-Solano A, Activation of coal tar pitch carbon fibres: physical activation vs. chemical activation. *Carbon* **42**:1367–1370 (2004). https://doi.org/10.1016/j.carbon.2004.01.013.
18 Shahcheragh SK, Bagheri Mohagheghi MM and Shirpay A, Effect of physical and chemical activation methods on the structure, optical absorbance, band gap and urbach energy of porous activated carbon. *SN Appl Sci* **5**:313 (2023). https://doi.org/10.1007/s42452-023-05559-6.
19 Alardhi SM, Albayati TM and Alrubaye JM, Adsorption of the methyl green dye pollutant from aqueous solution using mesoporous materials MCM-41 in a fixed-bed column. *Heliyon* **6**:e03253 (2020). https://doi.org/10.1016/j.heliyon.2020.e03253.
20 Lai KC, Tee WT, Yung N and Loh L, Continuous adsorption of Metanil yellow and Remazol black B dyes onto fixed-bed of 3D graphene oxide/chitosan biopolymer. *S Afr J Chem Eng* **48**:276–284 (2024). https://doi.org/10.1016/j.sajce.2024.02.007.
21 dos Santos DF, Moreira WM, de Araújo TP, Bernardo MMS, de Figueiredo Ligeiro da Fonseca IM, Ostroski IC *et al*., Competitive adsorption of acetaminophen and caffeine onto activated Tingui biochar: characterization, modeling, and mechanisms. *Environ Sci Pollut Res* **31**:53611–53628 (2023). https://doi.org/10.1007/s11356-023-31024-3.
22 Thommes M, Kaneko K, Neimark AV, Olivier JP, Rodriguez-Reinoso F, Rouquerol J *et al*., Physisorption of gases, with special reference to the evaluation of surface area and pore size distribution (IUPAC technical report). *Pure Appl Chem* **87**:1051–1069 (2015). https://doi.org/10.1515/pac-2014-1117.
23 Dias D, Lapa N, Bernardo M, Ribeiro W, Matos I, Fonseca I *et al*., Cr(III) removal from synthetic and industrial wastewaters by using co-gasification chars of rice waste streams. *Bioresour Technol* **266**:139–150 (2018). https://doi.org/10.1016/j.biortech.2018.06.054.
24 Quesada HB, De Araújo TP, Cusioli LF, De Barros MASD, Gomes RG and Bergamasco R, Evaluation of novel activated carbons from chichá-do-cerrado (Sterculia striata st. Hil. Et Naud) fruit shells on metformin adsorption and treatment of a synthetic mixture. *J Environ Chem Eng* **9**:104914 (2021). https://doi.org/10.1016/j.jece.2020.104914.
25 Herath A, Layne CA, Perez F, Hassan EB, Pittman CU and Mlsna TE, KOH-activated high surface area Douglas fir biochar for adsorbing aqueous Cr(VI), Pb(II) and Cd(II). *Chemosphere* **269**:128409 (2021). https://doi.org/10.1016/j.chemosphere.2020.128409.
26 Nguyen DT, Tran HN, Juang RS, Dat ND, Tomul F, Ivanets A *et al*., Adsorption process and mechanism of acetaminophen onto commercial activated carbon. *J Environ Chem Eng* **8**:104408 (2020). https://doi.org/10.1016/j.jece.2020.104408.
27 de Araújo TP, Quesada HB, dos Santos DF, da Silva Fonseca BC, Barbieri JZ, Bergamasco R *et al*., Acetaminophen removal by calcium alginate/activated hydrochar composite beads: batch and fixed-bed studies. *Int J Biol Macromol* **203**:553–562 (2022). https://doi.org/10.1016/j.ijbiomac.2022.01.177.
28 Chen WH, Wang CW, Ong HC, Show PL and Hsieh TH, Torrefaction, pyrolysis and two-stage thermodegradation of hemicellulose, cellulose and lignin. *Fuel* **258**:116168 (2019). https://doi.org/10.1016/j.fuel.2019.116168.
29 Halder P, Kundu S, Patel S, Parthasarathy R, Pramanik B, Paz-Ferreiro J *et al*., TGA-FTIR study on the slow pyrolysis of lignin and cellulose-rich fractions derived from imidazolium-based ionic liquid pretreatment of sugarcane straw. *Energy Convers Manage* **200**:112067 (2019). https://doi.org/10.1016/j.enconman.2019.112067.
30 Shahrokhi-Shahraki R, Benally C, El-Din MG and Park J, High efficiency removal of heavy metals using tire-derived activated carbon vs commercial activated carbon: insights into the adsorption mechanisms. *Chemosphere* **264**:128455 (2021). https://doi.org/10.1016/j.chemosphere.2020.128455.
31 Medellín-Castillo NA, González-Fernández LA, Ocampo-Pérez R, Leyva-Ramos R, Luiz-Dotto G, Flores-Ramírez R *et al*., Efficient removal of triclosan from water through activated carbon adsorption and photodegradation processes. *Environ Res* **246**:118162 (2024). https://doi.org/10.1016/j.envres.2024.118162.
32 Lima DR, Hosseini-Bandegharaei A, Thue PS, Lima EC, de Albuquerque YRT, dos Reis GS *et al*., Efficient acetaminophen removal from water and hospital effluents treatment by activated carbons derived from Brazil nutshells. *Colloids Surf, A* **583**:123966 (2019). https://doi.org/10.1016/j.colsurfa.2019.123966.
33 Khaksarfard Y, Bagheri A and Rafati AA, Synergistic effects of binary surfactant mixtures in the adsorption of diclofenac sodium drug from aqueous solution by modified zeolite. *J Colloid Interface Sci* **644**:186–199 (2023). https://doi.org/10.1016/j.jcis.2023.04.044.
34 Wong S, Lim Y, Ngadi N, Mat R, Hassan O, Inuwa IM *et al*., Removal of acetaminophen by activated carbon synthesized from spent tea leaves: equilibrium, kinetics and thermodynamics studies. *Powder Technol* **338**:878–886 (2018). https://doi.org/10.1016/j.powtec.2018.07.075.

35 Romero-Hernandez JJ, Paredes-Laverde M, Silva-Agredo J, Mercado DF, Ávila-Torres Y and Torres-Palma RA, Pharmaceutical adsorption on NaOH-treated rice husk-based activated carbons: kinetics, thermodynamics, and mechanisms. *J Cleaner Prod* **434**: 139935 (2024). https://doi.org/10.1016/j.jclepro.2023.139935.
36 Rey-mafull CA, Tacoronte JE, Garcia R, Tobella J, Llópiz JC and Iglesias A, Comparative study of the adsorption of acetaminophen on activated carbons in simulated gastric fluid. *SpringerPlus* **3**:48 (2014).
37 Yanan C, Srour Z, Ali J, Guo S, Taamalli S, Fèvre-Nollet V *et al*., Adsorption of paracetamol and ketoprofenon activated charcoal prepared from the residue of the fruit of Butiacapitate: experiments and theoretical interpretations. *Chem Eng J* **454**:139943 (2023). https://doi.org/10.1016/j.cej.2022.139943.
38 Oginni O, Singh K, Oporto G, Dawson-Andoh B, McDonald L and Sabolsky E, Influence of one-step and two-step KOH activation on activated carbon characteristics. *Bioresour Technol Rep* **7**:100266 (2019). https://doi.org/10.1016/j.biteb.2019.100266.
39 de Araújo TP, Quesada HB, Bergamasco R, Vareschini DT and de Barros MASD, Activated hydrochar produced from brewer's spent grain and its application in the removal of acetaminophen. *Bioresour Technol* **310**:123399 (2020). https://doi.org/10.1016/j.biortech.2020.123399.
40 Natarajan R, Banerjee K, Kumar PS, Somanna T, Tannani D, Arvind V *et al*., Performance study on adsorptive removal of acetaminophen from wastewater using silica microspheres: kinetic and isotherm studies. *Chemosphere* **272**:129896 (2021). https://doi.org/10.1016/j.chemosphere.2021.129896.
41 Medina FMO, Aguiar MB, Parolo ME and Avena MJ, Insights of competitive adsorption on activated carbon of binary caffeine and diclofenac solutions. *J Environ Manage* **278**:111523 (2021). https://doi.org/10.1016/j.jenvman.2020.111523.
42 Daikh S, Ouis D, Benyoucef A and Mouffok B, Equilibrium, kinetic and thermodynamic studies for evaluation of adsorption capacity of a new potential hybrid adsorbent based on polyaniline and chitosan for acetaminophen. *Chem Phys Lett* **798**:139565 (2022). https://doi.org/10.1016/j.cplett.2022.139565.
43 Islam MA, Nazal MK, Sajid M and Altahir SM, Adsorptive removal of paracetamol from aqueous media: a review of adsorbent materials, adsorption mechanisms, advancements, and future perspectives. *J Mol Liq* **396**:123976 (2024). https://doi.org/10.1016/j.molliq.2024.123976.
44 Al-Ghouti MA and Da'ana DA, Guidelines for the use and interpretation of adsorption isotherm models: a review. *J Hazard Mater* **393**:122383 (2020). https://doi.org/10.1016/j.jhazmat.2020.122383.
45 de Franco MAE, de Carvalho CB, Bonetto MM, de Pelegrini SR and Féris LA, Diclofenac removal from water by adsorption using activated carbon in batch mode and fixed-bed column: isotherms, thermodynamic study and breakthrough curves modeling. *J Cleaner Prod* **181**:145–154 (2018). https://doi.org/10.1016/j.jclepro.2018.01.138.
46 Inyinbor AA, Bankole DT, Adekola FA, Bello OS, Oreofe T, Amone K *et al*., Chemometrics validation of adsorption process economy: case study of acetaminophen removal onto quail eggshell adsorbents. *Sci Afr* **19**:e01471 (2023). https://doi.org/10.1016/j.sciaf.2022.e01471.
47 Veclani D, Tolazzi M, Fogolari F and Melchior A, Mechanism and thermodynamics of adsorption of diclofenac on graphene-based nanomaterials. *J Environ Chem Eng* **10**:108789 (2022). https://doi.org/10.1016/j.jece.2022.108789.
48 Xu R, Qin W, Tian Z, He Y, Wang X and Wen X, Enhanced micropollutants removal by nanofiltration and their environmental risks in wastewater reclamation: a pilot-scale study. *Sci Total Environ* **744**:140954 (2020). https://doi.org/10.1016/j.scitotenv.2020.140954.
49 Ye X, Li Y, Lin H, Chen Y and Liu M, Lignin-based magnetic nanoparticle adsorbent for diclofenac sodium removal: adsorption behavior and mechanisms. *J Polym Environ* **29**:3401–3411 (2021). https://doi.org/10.1007/s10924-021-02127-0.
50 Xie J, Liu M, He M, Liu Y, Li J, Yu F *et al*., Ultra-efficient adsorption of diclofenac sodium on fish-scale biochar functionalized with H3PO4 via synergistic mechanisms. *Environ Pollut* **322**:121226 (2023). https://doi.org/10.1016/j.envpol.2023.121226.
51 Patel M, Kumar R, Pittman CU and Mohan D, Ciprofloxacin and acetaminophen sorption onto banana peel biochars: environmental and process parameter influences. *Environ Res* **20**:111218 (2021). https://doi.org/10.1016/j.envres.2021.111218.

